Int. J. Solids Structures Vol. 26, No. 11, pp. 1211–1223, 1990
Printed in Great Britain.

0020-7683/90 $3.00 + .00

NUMERICAL RESULTS FOR TRANSFORMATION TOUGHENING IN CERAMICS

C. L. HOM and R. M. MCMEEKING
Department of Materials and Department of Mechanical Engineering,
University of California, Santa Barbara, CA 93106, U.S.A.

(*Received* 13 *July* 1989)

Abstract—Finite element analysis was used to study the fracture toughening of a ceramic by a stress-induced dilatant transformation of second phase particles. The finite element method was based on a continuum theory which modelled the composite as a subcritical material. Transient crack growth was simulated in the finite element mesh by a nodal release technique. The crack's remote tensile opening load was adjusted to maintain the near-tip energy release rate at the level necessary for crack advance. The transformation zone surrounding the crack developed as the crack propagated through the composite. Resistance curves were computed from the analysis; the results confirm that during crack advance maximum toughness is achieved before steady state is reached. Diagrams of each transformation zone and *R*-curve are provided to expedite comparison with experimental data.

INTRODUCTION

The fracture toughness of certain ceramics can be greatly enhanced by the presence of particles which undergo a stress-induced martensitic transformation (Evans and Heuer, 1980; Evans and Cannon, 1986; Green *et al.*, 1989) such as takes place in systems containing stabilized zirconia (ZrO_2) particles. Examples include partially stabilized zirconia (PSZ) and zirconia-toughened alumina (ZTA). At sufficiently high stress, the particles of such systems undergo a transformation from the tetragonal to the monoclinic phase which is accompanied by a volume increase of 4%. Since the transformation is stress induced, a zone of material containing transformed particles surrounds the crack tip after it has been stressed. The volume expansion of the particles in this zone will cause eigenstresses which will tend to close the crack and lower the stress intensity factor at the tip. This shielding mechanism means that a higher applied load than otherwise, and therefore an apparently higher stress intensity factor, is required to propagate the crack.

Transformation toughening was first modelled by McMeeking and Evans (1982) and Budiansky *et al.* (1983). The phenomenology of phase transformation was represented by the macroscopic hydrostatic stress versus dilatation strain behavior shown in Fig. 1. At the critical stress σ_m^c, phase transformation commences. If the slope $\bar{B}$ of the stress–strain curve during transformation is below $-4G/3$, where G is the shear modulus, then the transformation continues spontaneously and immediately to completion (Budiansky *et al.*, 1983). In fact, points on the stress–strain curve between 1 and 2 are excluded as unstable and the state jumps on transformation from 1 to the segment between 4 and 3. This situation has been termed supercritical. In the model of McMeeking and Evans, the phase

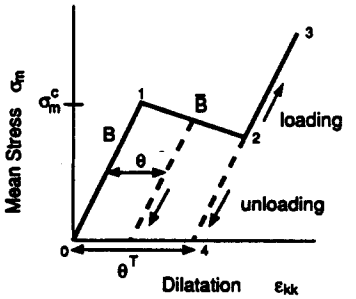

Fig. 1. The hydrostatic material behavior of a ceramic containing particles which undergo a stress-induced phase transformation.

transformation was supercritical and the volume increase due to transformation was asymptotically small. The transformation zones were also asymptotically small. By calculating the amount of crack tip shielding, they obtained estimates of the effective composite R-curve, the toughness value which rises as the crack grows. Eventually, a maximal steady-state toughness value develops after an amount of crack growth which is about three transformation zone widths.

Budiansky *et al.* (1983) considered supercritical and also subcritical materials in steady-state crack advance only. In the subcritical case, with $\bar{B} > -4G/3$, the phase change occurs gradually and the material can remain stably in a state in which the particles are only partially transformed. As a result, points in Fig. 1 between 1 and 2 are stable and the material moves gradually from 1 to 2 as strain increases. If the strain decreases (unloading) while the material is between 1 and 2, the state follows the line with slope B through the current location as shown in Fig. 1. In addition, Budiansky *et al.* also accounted accurately for the perturbation of the transformation zone size and shape due to the stresses induced by the transformation itself. Using finite element analysis, they calculated steady-state fracture toughnesses including cases where the volume increase from the transformation was quite large. Rose (1986) and Amazigo and Budiansky (1988) have provided additional analyses of steady-state toughening for dilatant transformations.

Stump and Budiansky (1989) have recently provided a more accurate estimate of the R-curve for a crack advancing in supercritically transforming material. The problems were solved numerically by means of an integral equation. The transformation zones evolved as the crack advanced and the remote load was adjusted to maintain the stress intensity factor at the critical constant value at the crack tip. Their solutions show that the maximum fracture toughness occurs after a finite amount of crack advance, and that this maximum can be significantly higher than the steady-state fracture toughness which develops later. The peak fracture toughness is associated with a transiently wider transformation zone. The result indicates that the amount of effective toughening is underestimated by the later steady-state value since the system must be forced to grow through the peak toughness state. The steady-state estimate generally underpredicts experimental data (Evans and Cannon, 1986) so the new predictions tend to bring the theory into better agreement. Furthermore, R-curves with peaks in the toughness have been reported by Swain (1983) and Swain and Hannink (1984).

The purpose of the calculations performed for this paper is to consider the transient behavior of a crack advancing in a material which transforms subcritically. Experimental evidence indicates that the transformation zones surrounding a crack tip tend to be diffuse or partially transformed, indicating a subcritical transformation. Finite element analysis is used to solve the problem of a semi-infinite crack growing in a transforming material under Mode I loading and plane strain conditions. Crack growth in the finite element mesh is modelled using a nodal release technique; the transformation zone develops as the crack advances. Resistance curves are computed for different purely dilatant transformation strains and the results are compared with the steady-state analysis of Budiansky *et al.* (1983). A near critical case almost equivalent to the supercritical analysis by Stump and Budiansky (1989) was also analyzed for comparison. Extensive documentation of each solution is provided so that comparisons with experimental data can be made more easily.

CONSTITUTIVE RELATIONS

In this section we describe the constitutive relations used to model transformation toughened composites. Developed by Budiansky *et al.* (1983), the model assumes that the transformation zone contains many particles and thus a continuum description of the composite can be formulated. The composite material is isotropic and consists of a linear elastic isotropic matrix containing linear elastic isotropic particles which undergo an irreversible dilatant transformation.

Since the transformation is purely dilatant, the macroscopic shear response is entirely linear elastic with modulus G, which will depend on the composite properties of the material.

Thus the deviatoric stress–strain relationship for the composite is

$$\sigma'_{ij} = 2G\varepsilon'_{ij} \tag{1}$$

where σ' is the deviatoric part of the macroscopic stress and ε' is the deviatoric part of the macroscopic strain.

The dilatant behavior of the composite is depicted in Fig. 1, and can be represented by

$$\varepsilon_{kk} = \frac{\sigma_m}{B} + \theta \tag{2}$$

where ε_{kk} denotes the total dilatation; σ_m is the hydrostatic part of the stress equal to $\sigma_{kk}/3$; B is the bulk modulus for the material; and θ is the current dilatation due to particle transformation in a macroscopic element of the composite material. (Einstein summation is used on repeated indices throughout.)

When the strain $\varepsilon^c_{kk} = \sigma^c_m/B$ is exceeded, locally particles change phase to some extent. When all of the particles have transformed locally, the macroscopic dilatation θ is equal to θ^T. In a material in which the elastic moduli of the particles are identical with those of the matrix $\theta^T = c\theta^T_p$, where c is the volume fraction of particles and θ^T_p is the free dilatation of an individual particle (4% in the case of zirconia) (Budiansky *et al.*, 1983). However, McMeeking (1986) has shown that in binary elastic composites, $\theta^T = Fc\theta^T_p$, where F is a factor which depends on the ratios of elastic moduli.

When the material is partially transformed into subcritical materials, the incremental dilatation during loading ($\varepsilon_{kk} > 0$) and due to transformation is (Budiansky *et al.*, 1983).

$$\dot{\theta} = (1 - \bar{B}/B)\dot{\varepsilon}_{kk} \tag{3}$$

when

$$\sigma^c_m/B + \theta(1 - \bar{B}/B) \leqslant \varepsilon_{kk} \leqslant \sigma^c_m/B + \theta^T(1 - \bar{B}/B).$$

Since the phase transformation is assumed irreversible, θ remains constant during unloading ($\varepsilon_{kk} < 0$) in all cases. In the critical and supercritical case, eqn (3) is replaced by

$$\mathrm{d}\theta/\mathrm{d}\varepsilon_{kk} = \theta^T \delta_D(\varepsilon_{kk} - \sigma^c_m/B) \tag{4}$$

where δ_D is a Dirac delta function.

BOUNDARY VALUE PROBLEM

The problem of a very long crack growing in plane strain with a very small zone of phase transforming particles (see Fig. 2) was solved using the finite element method.

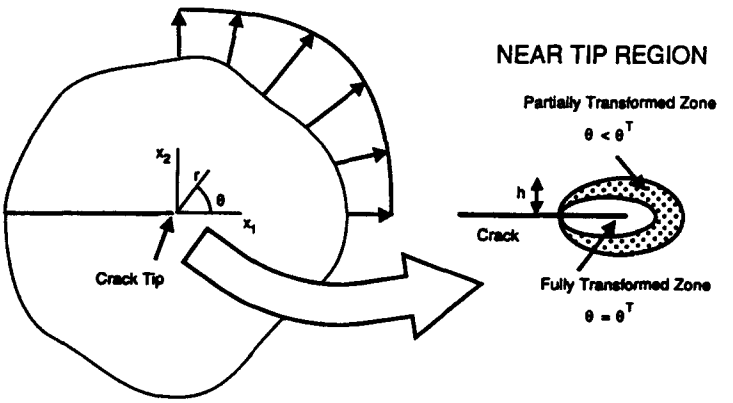

Fig. 2. The boundary value problem of a semi-infinite crack subject to a mode I tensile opening load.

Displacement boundary conditions corresponding to a Mode I linear elastic plane strain field were applied around the outer perimeter of the domain. The magnitude of the applied load is characterized by K^{APP}, the Mode I elastic stress intensity factor. As shown in Fig. 2, material near the tip transforms due to the stress intensification generated by the crack. A zone of material which has completely transformed ($\theta = \theta^T$) surrounds the crack tip. This core region is incrementally linear elastic with a permanent residual strain. Consequently, the stress field at the crack tip has an $r^{-1/2}$ singularity and is characterized by a stress intensity factor K^{TIP}. In the subcritical case, the region of purely transformed material is surrounded by a zone of material which is partially transformed ($\theta < \theta^T$). In the critical and supercritical cases, partially transformed material does not exist and θ jumps from zero to θ^T across the zone perimeter.

For a stationary crack with monotonically increasing K^{APP} no unloading occurs and the J-integral of Rice (1968) is path independent (Budiansky *et al.*, 1983). As a result, $K^{TIP} = K^{APP}$ and thus, prior to any crack growth, there is no shielding (McMeeking and Evans, 1982; Budiansky *et al.*, 1983). The crack will commence growing when $K^{TIP} = K^C$, the fracture toughness of the composite in the crack tip state, i.e. with pretransformed particles. Equivalently, crack growth commences when $K^{APP} = K^C$.

As the crack propagates and a wake of transformed material develops, K^{TIP} decreases compared to K^{APP} due to shielding. To maintain crack growth, K^{APP} must be continually adjusted so that K^{TIP} equals K^C. K^{APP} is the effective fracture toughness of the composite material and the R-curve is its graph versus the amount of crack growth Δa.

Finally, all length scales in the moving crack tip problem were normalized by L, where L is defined by

$$L = \frac{2}{9\pi}\left[\frac{K^c(1+\nu)}{\sigma_m^c}\right]^2. \tag{5}$$

Physically, L is the distance on the X_1-axis from the tip ahead to the boundary of the nominal transformation zone for the stationary crack with $K^{APP} = K^C$. The solutions depend on the strength of the transformation which is characterized by the nondimensional parameter ω, where

$$\omega = \frac{E\theta^T}{\sigma_m^c}\left[\frac{1+\nu}{1-\nu}\right]. \tag{6}$$

FINITE ELEMENT SOLUTIONS

The finite element method used to solve these problems has been described by Hom *et al.* (1989). The method was incremental with the load, K^{APP}, adjusted in steps as necessary to tend to maintain K^{TIP} equal to K^C. After each adjustment of the load, a successive approximation iteration was carried out until satisfactory convergence of the solution was achieved. When K^{TIP} equaled K^C, the crack tip node was released incrementally to advance the crack, with iterations carried out as necessary. Thereafter, K^{APP} was again adjusted in steps to return K^{TIP} to K^C and so on. The virtual crack extension method of Parks (1974, 1978) was used to calculate K^{TIP} when necessary. The finite element mesh in Fig. 3 was used for the calculations. The crack was grown from the point marked "STATIONARY CRACK TIP" in that figure to near the point marked "MOVING CRACK TIP".

Attempts were made to compute results for the precisely critical case ($\bar{B} = -4G/3$). However, it was found that the iterative procedure failed to converge. Without any change to the load or geometry, the transformation zone simply expanded with each iteration. Thus, no stable transformation zone size was ever established even for stationary cracks. No way was found by us to avoid this in the algorithm directly. Instead, subcritical materials were analyzed. Satisfactory convergence to a rather strict criterion was then achieved. Few iterations were required when $\bar{B}$ equaled zero but considerably more were necessary when $\bar{B}$ was smaller.

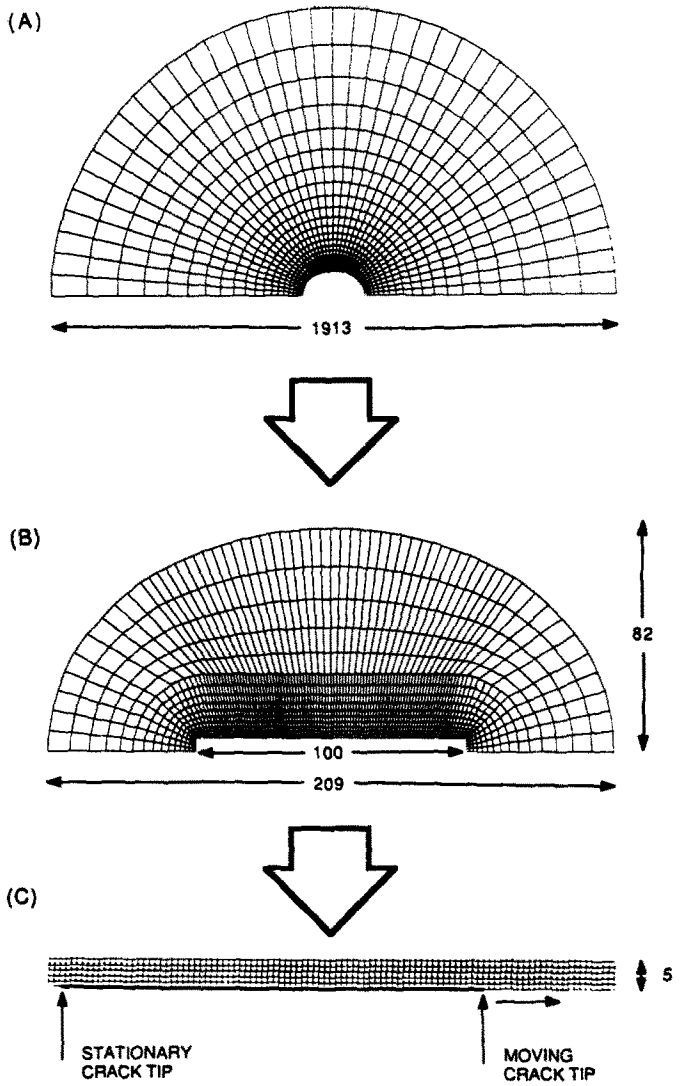

Fig. 3. The finite element mesh used to examine a growing crack in a transformation-toughened composite.

The subcritical results we obtained involved partially transformed material within the zone. However, as $\bar{B}$ approached $-4G/3$, the regions of partially transformed material formed a narrow band around the outer perimeter of the zone. For a sufficiently small value of $\bar{B}$ and with appropriate choices of other parameters, this band was made narrower than the distance between two neighboring integration stations in the finite element mesh. Thus, at one integration station the material is untransformed and at the neighboring integration station across the partially transformed band, the material is completely transformed. This situation is as good as can be achieved anyway for the exactly critical material given the discreteness of the mesh. The near critical case so calculated is numerically equivalent to the exactly critical case for the given mesh. This equivalence was actually achieved for $\omega = 5$ with $\bar{B} = -1.3G$ in the mesh shown in Fig. 3. This solution was slow to converge (~ 50 iterations per step compared to five for $\bar{B} = 0$) and the amount of computer time precluded us from carrying out other near critical solutions.

The parameters of the problems were chosen so that at least 10 elements spanned the transformation zone in the X_2 direction. To check if the mesh layout was fine enough, σ_m^c was made smaller to enlarge the zone, making L larger, equivalent to refining the mesh. The combination $E\theta^T$ was reduced also to keep ω fixed. The results of calculations then carried out were identical to those performed in the effectively coarser mesh, confirming that the mesh and calculation strategy were satisfactory.

RESULTS FOR A GROWING CRACK

The problem of a crack in untransformed material growing and creating a transformation zone was solved for various material parameters. These characteristic parameters are the transformation strength ω, Poisson's ratio ν (taken to be 0.3 throughout) and $\bar{B}/G$. Three sets of finite element computations were done with $\omega = 5$, 10 and 15. In each set of calculations, cases were run for $\bar{B}/G = 0$, -0.5 and -1.0. The calculation with $\omega = 5$ and $\bar{B}/G = -1.3$ was also done for comparison with the calculations of Stump and Budiansky (1989). In all cases the crack was propagated a distance of at least $8L$.

Transformation zones

The transformation zone for the near critical case ($\bar{B}/G = -1.3$) with $\omega = 5$ and $\Delta a = 11.4L$ is shown in Fig. 4. In this case, the layer of partially transformed material is very thin and has not been shown in the figure. It is thinner than the distance between neighboring integration stations in the finite element mesh—about 10% of the peak zone height above the crack, h, shown in Fig. 4. Apart from this thin layer, the material inside the zone has transformed completely. It is clear from the zone shape, that as the crack grew, the zone first widened sharply and then gradually. After reaching a maximum width, the zone narrowed sharply with growth and then appears to settle into a steady state.

In this case, the maximum zone height is $h_m = 1.06L$ and occurs after the crack has grown a distance $3.7L$. The finite element results show that the zone reaches a steady-state height of $0.88L$. The transient behavior of a crack growing in a supercritical material has also been considered by Stump and Budiansky (1989). For $\omega = 5$, their results show that the maximum zone height is $1.03L$ and occurs when $\Delta a = 2.4L$. Their computation also predicts a steady-state zone height of $0.89L$. Overall, the zones have very similar shapes. It should be noted that between $\Delta a = 2.4L$ and $3.7L$, the zone height is almost steady, and the discrepancy in the position of the zone width peak should be considered in that context.

The development of the transformation zone for the case $\bar{B}/G = 0$ and $\omega = 10$ as the crack tip moves to the right is shown in Fig. 5. The zone is shown for different crack lengths, where Δa is the amount of growth which has taken place. The zones are depicted as contour plots of the transformation dilatation θ. As expected the crack tip is surrounded by a region of fully transformed material which in turn is surrounded by a region of partially transformed material. As the crack grows, the zone expands in height. The height of the zone h reaches a maximum at $1.02L$ after the crack has propagated a distance $1.7L$. Thereafter, the zone narrows and when the crack reaches a steady state at around $\Delta a = 8L$, the zone height in the steady-state region is smaller at $0.88L$. The steady-state zone height predicted by Budiansky *et al.* (1983) for subcritical material with $\bar{B}/G = 0$ and $\omega = 10$ is $h = 0.84L$.

Figure 6(a) shows the transformation zone when $\bar{B}/G = 0$ and $\omega = 5$ after the crack has propagated a distance of $8.6L$. The fully transformed region in this case is larger than the fully transformed region for the $\omega = 10$ case. However, the whole transformation region observed for $\omega = 5$ is smaller than for $\omega = 10$, and the peak height is not as large. In this case h reaches a maximum of $0.87L$ after the crack has propagated a distance $1.4L$.

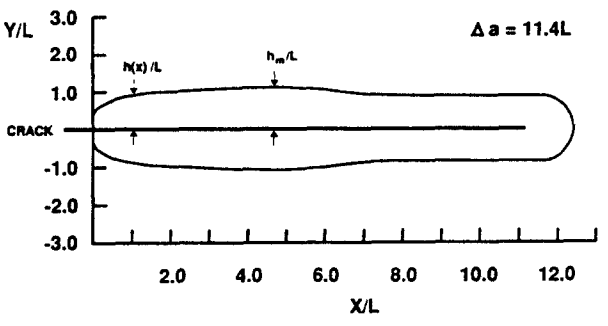

Fig. 4. Transformation zone for the case $\omega = 5$ and $\bar{B}/G = -1.3$ when $\Delta a = 11.4L$.

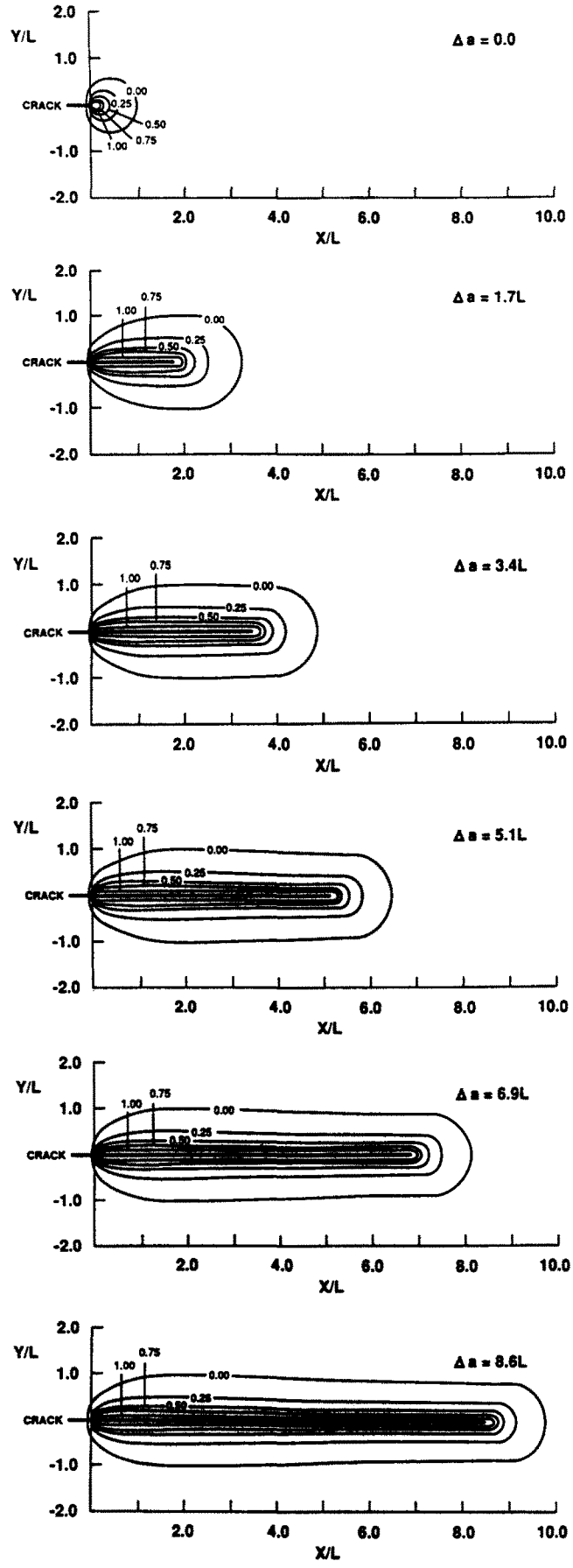

Fig. 5. Development of the transformation zone for the case $\omega = 10$ and $\bar{B}/G = 0$ as the crack grows; Δa is the amount of crack growth. Contour levels are for θ/θ^{T}.

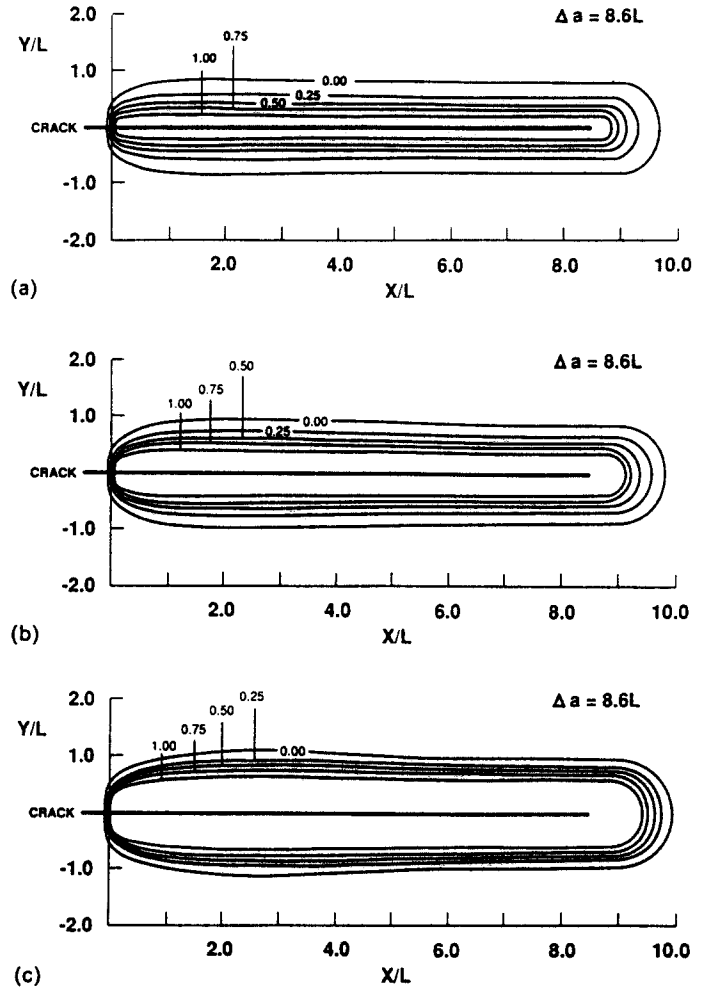

Fig. 6. Transformation zone contour plots of θ/θ^T for the case of $\omega = 5$ when $\Delta a = 8.6L$. (a) $\bar{B}/G = 0$, (b) $\bar{B}/G = -0.5$, (c) $\bar{B}/G = -1.0$.

The steady-state zone height predicted by the finite element calculations is $0.81L$. The computations of Budiansky *et al.* (1983) predicted the steady-state zone height as $0.89L$. The transformation zones after the crack has propagated a distance $8.6L$ for $\omega = 5$ with $\bar{B}/G = -0.5$ and -1.0 are shown in Figs 6(b) and 6(c), respectively. It can be seen clearly that for the smaller values of $\bar{B}$ there is a larger fully transformed zone compared to the total zone size. The next figure in this series for $\omega = 5$ is that in Fig. 4 for $\bar{B}/G = -1.3$ discussed already where there is no partially transformed zone.

Figures 7(a) and (b) are plots of the transformation zone after the crack has propagated a distance $8.6L$ for $\omega = 10$ when $\bar{B}/G = -0.5$ and -1.0, respectively. Comparison of Figs 7 with 6 shows that a larger relative dilatation ω produces a larger final zone size even though they start growing from nearly the same initial zone size. Finally, Figs 8(a,b,c) show the transformation zones after the crack has propagated a distance $12.9L$ for the cases when $\omega = 15$.

Table 1 shows the peak and steady-state zone heights and Δa when the peak occurs for each case calculated. The finite element results show that for a given L, the peak height and the steady-state zone height are larger for stronger transformation strengths ω. Also, the crack must propagate further to reach both the maximum zone height and the steady-state zone height for larger ω. Similarly, the closer $\bar{B}$ is to the critical value of $-4G/3$, the larger is the peak zone height and the steady height. The latter comment applies except for the near critical case $\bar{B}/G = -1.3$ where the trend seems to reverse. But when the material is near critical, the distance the crack must propagate to achieve both the maximum zone

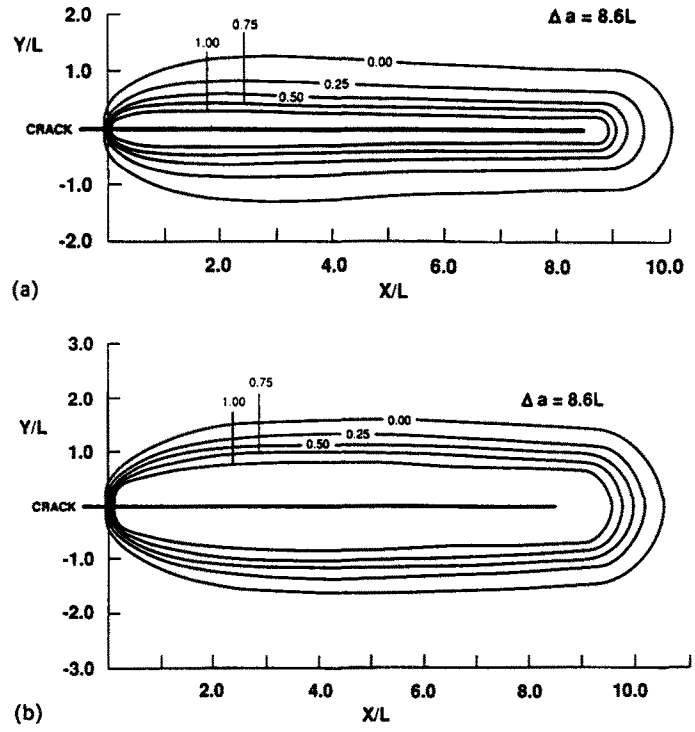

Fig. 7. Transformation zone contour plots of θ/θ^T for the case of $\omega = 10$ when $\Delta a = 8.6L$. (a) $\bar{B}/G = -0.5$, (b) $\bar{B}/G = -1.0$.

height and the steady state is greater. Included in Table 1 for completeness are results taken from Stump and Budiansky (1989) for the supercritical material.

Resistance curves

As mentioned earlier, the remote applied stress intensity factor was varied during crack advance to maintain $K^{TIP} = K^C$ at the crack tip. The R-curves (K^{APP} verses Δa) for the case when $\omega = 5$ are shown in Fig. 9. As expected, in each case the transformation zone shields the crack tip and toughening is observed. The R-curves rise to a peak level associated with the widest part of the zone. Thereafter, the R-curve falls as the zone narrows. The curves then tend to settle down to a steady state. The relative amount of toughening is higher for the lower values of $\bar{B}$ because there is relatively more fully transformed material in the wake zone. In addition, the peak toughening relative to the later steady-state value is more pronounced when $\bar{B}$ is more negative.

After the crack has propagated a sufficient distance, the R-curve approaches an asymptotic value. This steady-state value of K^{APP} corresponds to the steady-state region in the transformation zone. For comparison, the dashed lines in Fig. 9 denote the toughnesses

Table 1. Zone heights and fracture toughnesses predicted by the finite element analysis for subcritical material. Results for $\bar{B}/G = -4/3$ are from Stump and Budiansky (1989).

ω	5	5	5	5	5	10	10	10	10	15	15	15	15
$\bar{B}/G$	0.0	−0.5	−1.0	−1.3	−4/3	0.0	−0.5	−1.0	−4/3	0.0	−0.5	−1.0	−4/3
Δa for peak h	1.4L	1.8L	2.1L	3.7L	2.4L	1.7L	2.2L	3.7L	5.6L	1.9L	2.7L	6.4L	18.4L
Peak h	0.87L	0.95L	1.12L	1.06L	1.03L	1.02L	1.29L	1.67L	1.91L	1.17L	1.69L	2.94L	5.17L
Steady-state h	0.81L	0.85L	0.97L	0.88L	0.89L	0.88L	1.05L	—	1.21L	0.97L	1.17L	—	1.73L
Δa for peak K_{APP}/K_C	2.9L	3.8L	4.5L	5.6L	5.5L	2.7L	3.9L	6.5L	10.3L	3.1L	4.4L	10.6L	29.4L
Peak K_{APP}/K_C	1.19	1.23	1.27	1.30	1.29	1.34	1.46	1.65	1.80	1.48	1.70	2.24	3.07
Steady-state K_{APP}/K_C	1.19	1.22	1.26	1.27	1.26	1.33	1.43	—	1.63	1.46	1.62	—	2.15

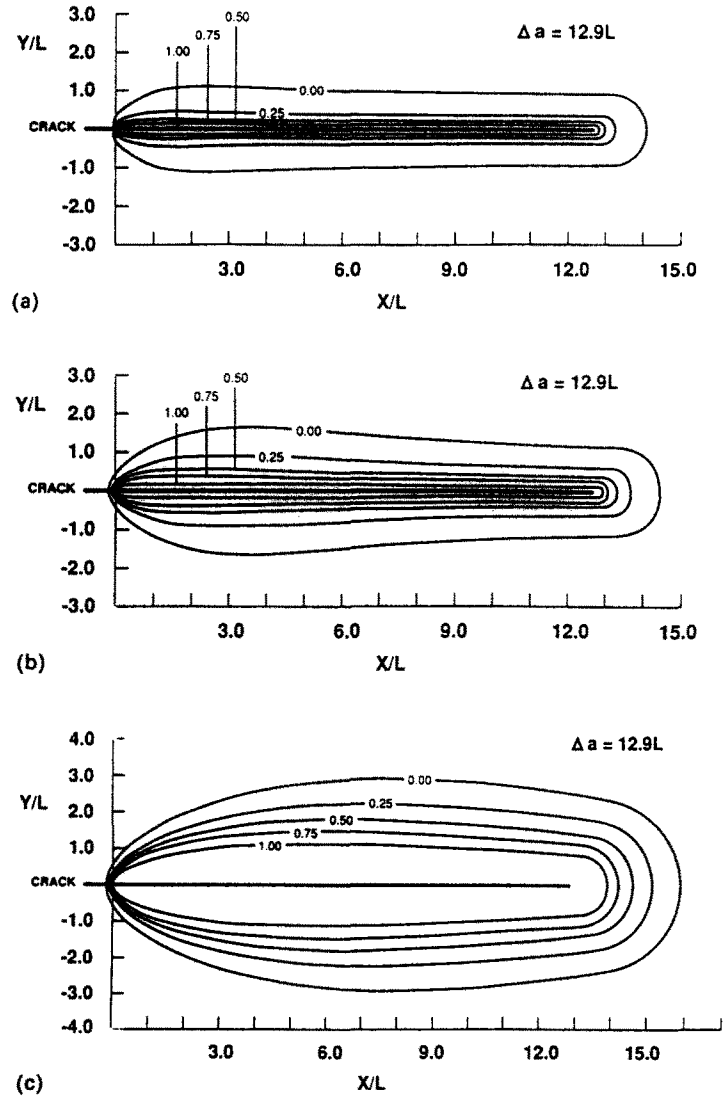

Fig. 8. Transformation zone contour plots of θ/θ^T for the case of $\omega = 15$ when $\Delta a = 12.9L$. (a) $\bar{B}/G = 0$, (b) $\bar{B}/G = -0.5$, (c) $\bar{B}/G = -1.0$.

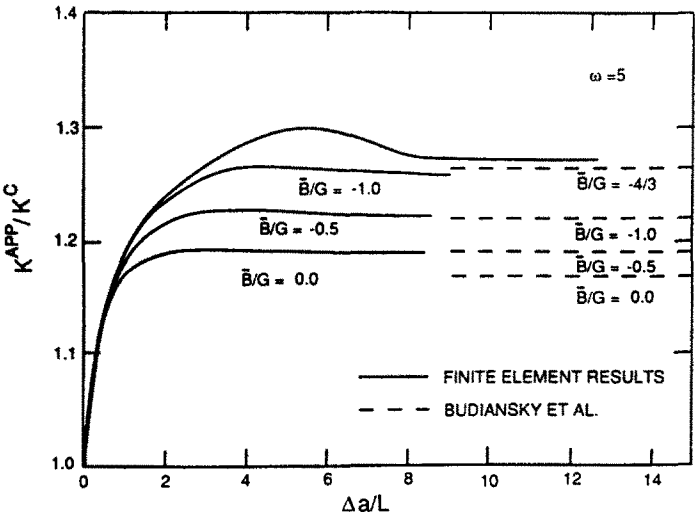

Fig. 9. Resistance curves for the cases of $\omega = 5$. The steady-state results of Budiansky *et al.* (1983) are shown with dashed lines.

predicted by the steady-state finite element analyses of Budiansky *et al.* (1983). The steady-state toughness for the near critical material $\bar{B}/G = -1.3$ predicted by our finite element calculation agrees well with the steady-state analysis for critical and supercritical materials which is exact. Furthermore, the peak toughness agrees well with the result of Stump and Budiansky (1989). These results give us confidence in our numerical solutions. For the near critical case ($\bar{B}/G = -1.3$) with $\omega = 5$, our finite element analysis predicts a maximum and steady-state K^{APP} of $1.30K^C$ and $1.27K^C$, respectively. The peak in K^{APP} occurs when the crack has grown a distance $5.6L$. For the supercritical material, Stump and Budiansky (1989) predict a toughness value of $1.29K^C$ for the peak and the steady-state value is $1.26K^C$ (Budiansky *et al.*, 1983). Therefore, the zone contributions to toughness agree to within a few per cent. Maximum K^{APP} in the results of Stump and Budiansky (1989) occurred when $\Delta a = 5.5L$.

The subcritical steady-state values of K^{APP} predicted by our transient finite element analysis are higher than the steady-state values of Budiansky *et al.* (1983). For example, when $\bar{B} = 0$ the steady-state toughness predicted by the finite element analysis is $1.19K^C$ while the analysis of Budiansky *et al.* (1983) predicts $1.17K^C$. This means that our prediction of the zone contribution is about 10% higher. The difference is unresolved.

For the subcritical material, the differences in the peak and steady-state toughnesses are much smaller than the supercritical case. For $\bar{B} = 0$ the finite element analysis shows that both the peak and steady-state K^{APP} are indistinguishable at $1.19K^C$. Even for $\bar{B}/G = -1.0$, the peak K^{APP} is only $1.27K^C$ compared to a steady-state value of $1.26K^C$.

Figure 10 shows the R-curves for the case when $\omega = 10$. Because the strength of the transformation is greater, the toughnesses computed in these cases are higher than those for $\omega = 5$. Also, the peak value for K^{APP} is more pronounced compared to the steady-state value of K^{APP}. For $\bar{B}/G = -1.0$, the computation was only carried out until $\Delta a = 8.6L$ and a steady state was not developed. However, a peak value of K^{APP} of $1.65K^C$ was calculated. The dashed lines in Fig. 10 indicate the results of Budiansky *et al.* (1983). As in the case of $\omega = 5$, the steady-state toughnesses predicted by our finite element analyses for $\omega = 10$ are higher than those of the previous steady-state analysis. The R-curves for $\omega = 15$ are shown in Fig. 11. The higher toughnesses reflect the greater strength of the transformation. Again, the steady-state toughnesses were higher than those predicted by Budiansky *et al.* (1983).

In addition to zone shape information, Table 1 shows the peak and steady-state toughnesses and Δa to reach peak toughness predicted by our finite element analysis for all cases examined in this study. The numerical computations show that larger peak and steady toughnesses are achieved when ω is greater and $\bar{B}$ is closer to critical, i.e. a stronger

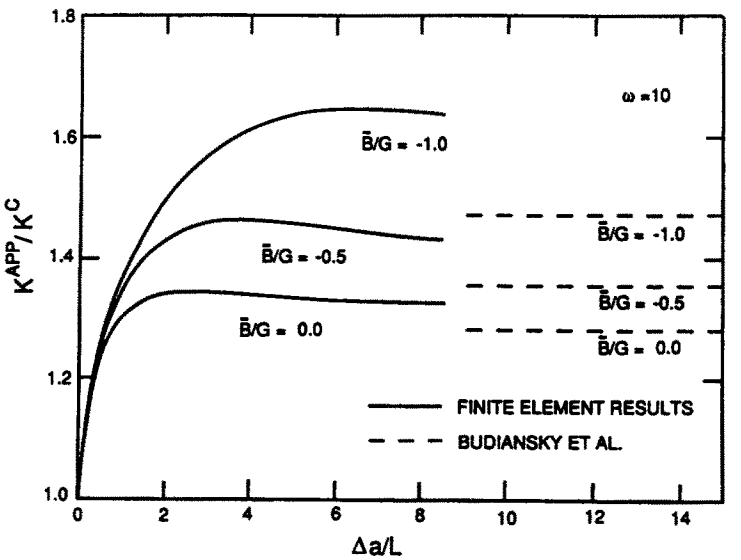

Fig. 10. Resistance curves for the cases of $\omega = 10$. The steady-state results of Budiansky *et al.* (1983) are shown with dashed lines.

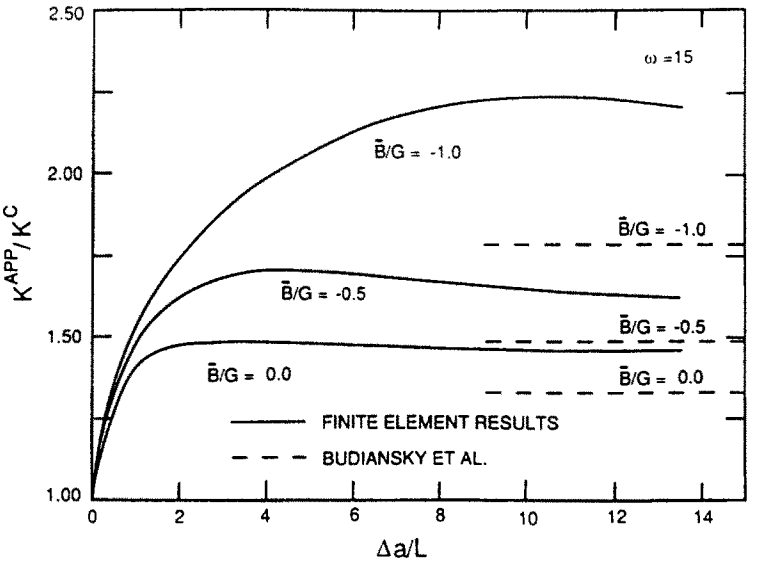

Fig. 11. Resistance curves for the cases when $\omega = 15$. The steady-state results of Budiansky *et al.* (1983) are shown with dashed lines.

transformation with more material fully transforming. Also, with increasing ω and $\bar{B}$ closer to critical, the crack must grow a greater distance in terms of L to reach both the peak toughness and the steady-state.

DISCUSSION

The finite element results presented in this paper indicate agreement between our near critical solution and the accepted steady-state toughening estimate of previous work (McMeeking and Evans, 1982; Budiansky *et al.*, 1983; Stump and Budiansky, 1989). In addition, the peak toughness predicted here for the near critical case by finite elements agrees with the value obtained by Stump and Budiansky (1989) by another method. This gives us confidence in our numerical results. It is worth noting that we have achieved agreement with other results in the case in which we found convergence most difficult to obtain, i.e. the near critical situation.

In contrast, it is found that our predictions for steady-state behavior of subcritical materials disagree with the established results of Budiansky *et al.* (1983). We have checked to see if lack of mesh refinement is the source of our problem, but that is not so. The discrepancy remains unresolved.

Our calculations confirm the novel R-curve behavior found by Stump and Budiansky (1989) in their calculations, namely that there is a peak in toughness prior to steady state. Since the peak of the R-curve will determine the potential toughness of the material, these new higher theoretical values are significant. The actual toughness measured in an experiment will depend on the compliance of the system (McMeeking and Evans, 1982) and this must be taken into account. However, it is interesting that theory has so far underpredicted experiments on transformation toughening (Evans and Cannon, 1986) and so the new results offer the prospect of the theory being brought into better agreement with the data.

It has also been observed that the original very approximate prediction of an R-curve by McMeeking and Evans (1982) has proved to be too stiff compared to the data (Heuer, 1987). It is likely that the R-curves now predicted by Stump and Budiansky (1989) and Hom and McMeeking will tend to rectify this situation. Compared to the original R-curve predicted by McMeeking and Evans (1982), those calculated in this case for $\omega = 5$ as well as that of Stump and Budiansky (1989) are more compliant. For higher values of ω, the new calculated R-curves are even more compliant so that the difference from the old curve of McMeeking and Evans (1982) will be greater.

A note of caution is called for, however. The ratio of Δa for peak K_{APP}/K_C divided by peak h is typically in the range 3–5 (see Table 1). Thus, the amount of crack growth to reach peak toughness is only about 3–5 times the observed fully developed zone height. This range is not very different from the original prediction (McMeeking and Evans, 1982) that the R-curve would peak at about three zone heights.

It should be noted also that all the results obtained so far are for transformation zones which are very small compared to specimen dimensions. No allowance has been made for large-scale transformation.

Acknowledgements—The authors would like to thank A. G. Evans for many helpful discussions and comments on this paper. This work was supported by the DARPA University Research Initiative under ONR contract N00014-86-K-0753. The calculations were carried out on a Convex C1-XP2 computer.

REFERENCES

Amazigo, J. C. and Budiansky, B. (1988). Steady-state crack growth in supercritically transforming materials. *Int. J. Solids Structures* **24**, 751–755.

Budiansky, B., Hutchinson, J. W. and Lambropoulos, J. C. (1983). Continuum theory of dilatant transformation toughening in ceramics. *Int. J. Solids Structures* **19**, 337–355.

Evans, A. G. and Cannon, R. M. (1986). Toughening of brittle solids by martensitic transformations. *Acta Metall.* **34**, 761–800.

Evans, A. G. and Heuer, A. H. (1980). Review—Transformation toughening in ceramics: martensitic transformations in crack tip stress fields. *J. Am. Ceram. Soc.* **63**, 241–248.

Green, D. J., Hannink, R. H. J. and Swain, M. V. (1989). *Transformation Toughening of Ceramics*. CRC Press, Boca Raton, FL.

Heuer, A. H. (1987). Transformation toughening in ZrO_2-containing ceramics. *J. Am. Ceram. Soc.* **70**, 689–698.

Hom, C. L., Mataga, P. A. and McMeeking, R. M. (1989). Some recent developments in numerical modelling of fracture toughness in brittle matrix composites. *Int. J. Num. Methods Engng.* **27**.

McMeeking, R. M. (1986). The effective transformation strain in binary elastic composites. *J. Am. Ceram. Soc.* **69**, C301–302.

McMeeking, R. M. and Evans, A. G. (1982). Mechanics of transformation toughening in brittle materials. *J. Am. Ceram. Soc.* **65**, 242–246.

Parks, D. M. (1974). A stiffness derivative finite element technique for determination of crack tip stress intensity factors. *Int. J. Fract.* **10**, 487–502.

Parks, D. M. (1978). *Numerical Methods in Fracture Mechanics* (Edited by A. R. Luxmore and D. R. J. Owen), pp. 464–478. Pineridge Press, Swansea, U.K.

Rice, J. R. (1968). A path independent integral and the approximate analysis of strain concentrations by notches and cracks. *Trans. ASME* **80**, Series E, *J. Appl. Mech.* **35**, 379–386.

Rose, L. R. F. (1986). The size of the transformed zone during steady-state cracking in transformation-toughened materials. *J. Am. Ceram. Soc.* **34**, 208–211.

Stump, D. M. and Budiansky, B. (1989). Crack growth resistance in transformation-toughened ceramics. *Int. J. Solids Structures* **25**, 635–646.

Swain, M. V. (1983). *Fracture Mechanics of Ceramics* (Edited by R. C. Bradt *et al.*), Vol. 6, pp. 355–370. Plenum, London and New York.

Swain, M. V. and Hannink, R. H. J. (1984). *Fracture Mechanics of Ceramics* (Edited by N. Claussen), Vol. 12, pp. 225–239. Plenum, London and New York.